ACS Catalysis

Research Article

pubs.acs.org/acscatalysis

Application of a Heme-Binding Protein Eluted from Encapsulated Biomaterials to the Catalysis of Enantioselective Oxidation

Hiroyuki Nagaoka*

Sanyo Shokuhin Co., Ltd. R & D, 555-4 Asakura, Maebashi, Gunma 371-0811, Japan

Supporting Information

ABSTRACT: A protein complex (PX) eluted from an encapsulated pea protein (PP) under aeration can be used as two types of biocatalysts: a polyethylene glycol (PEG) (1000/4000 = 2/1)-aggregated PX (AGPX) and a glutaraldehyde (GA)/compound-modified PX (CMPX). These biocatalysts have the following functional activities: AGPX can catalyze the oxidation of *rac*-1-(6-methoxynaphthalen-2-yl)ethanol (*rac*-**1**) to the corresponding ketone (~95% chemical yield) via the selective oxidation of (*S*)-(+)-**1**, leaving highly enantiopure (*R*)-(−)-**1** (>99% ee; ~50% chemical yield); CMPX can catalyze the kinetic resolution of (*S*)-(+)-**1** ((*S*)-naproxen precursor, >99% ee, ~50% chemical yield) via the selective oxidation of (*R*)-(−)-**1** to the corresponding ketone. Both reactions occur in the absence of an added cofactor (e.g., NAD(P)) in aqueous media. The specific activities of AGPX and CMPX were determined to be 0.8 ± 0.03 mU (mean ± SD) and 0.6 ± 0.02 mU (mean ± SD), respectively, and the exact nature of the species engaged in the key reaction was consistent with that of a heme-binding protein (HBP), on the basis of an N-terminal sequence comparison, which showed 93% similarity with a 20.853 kDa hemophore HasA gene product [*Pseudomonas fluorescens Pf-5*, a plant commensal bacterium]. PP-HBP can be regenerated via successive asymmetric catalytic events using an incorporated iron electron-transfer system ($Fe^{2+} \rightleftarrows Fe^{3+}$) in the presence of oxygen, a process seemingly similar to that utilized by hemoglobin. The use of a raw biomaterial as a PX-catalytic system with an incorporated redox cofactor for asymmetric oxidation overcomes the apparent difficulties in working with pure dehydrogenase enzyme/redox cofactor systems for biotransformation.

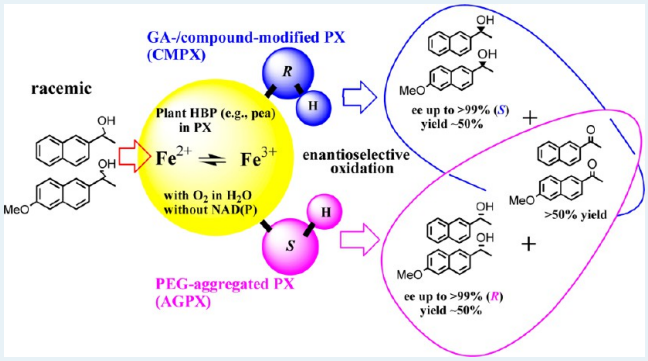

KEYWORDS: *heme-binding protein, hemophore, asymmetric oxidation, iron electron-transfer system, plant HBP, oxygen dependence*

INTRODUCTION

A review covering the well-known alcohol dehydrogenase (ADH) enzyme system that incorporates redox cysteine disulfide bonds, redox zinc, and a redox cofactor (such as NAD(P) or FAD) has been published,[1] and the high cost and instability of redox cofactors in enzymatic synthesis justifies efforts to regenerate them.[2] On the other hand, the use of heme-binding proteins (HBPs), which incorporate an iron-electron-transfer system for the asymmetric oxidation (with oxygen) of secondary alcohols in organic synthesis, has not been published, although the use of such a system overcomes the apparent difficulties in working with pure dehydrogenase enzyme/redox cofactor systems for microbial biotransformation. It has been reported, however, that a hydrogen peroxide-driven cytochrome P450 enzyme (e.g., $P450_{BS\beta}$, a HBP) that depends on oxygen instead of a redox cofactor (NAD(P)H)[3a−c] as a detoxification system catalyzes hydroxylation, epoxidation, and dehalogenation, generating a reactive oxygen species via an iron-electron-transfer system,[3d] and that cytochrome *c* oxidase (CytcO, a HBP)[3e] incorporates the electron-transfer system for the reduction of oxygen to water to enable proton pumping across cell membranes.[3f] Furthermore, the hemophore HasA secreted by host HBPs (e.g., ABC transporters, CytcO, and P450)[4a] enables heme uptake across the cell outer membrane and spontaneously transforms it into the HasR receptor at the heme-binding site.[4b] Cytochrome P450 enzymes are found in all organisms, and compared with bacteria HBP and animal HBP (P450: ~20 and 60 different forms, respectively), plants make several forms because they synthesize unusual pigments and exotic toxins to protect themselves;[4d] thus, the development of a new method for the purification and characterization of a new plant-HBP system may be enabled.

The use of biomaterials as protein complex (PX)-catalytic systems incorporating redox cofactors for asymmetric oxidation/reduction reactions has been studied previously.[5] In particular, the PX eluted from biomaterials (i.e., pea protein (PP)) encapsulated with calcium alginate gel (PP gel) is available for the synthesis and enantiomeric resolution of m- and p-substituted racemic aryl methyl carbinols.[6] Other biomaterials used instead of proteins include young wheat or

Received: September 3, 2013
Revised: December 24, 2013
Published: January 7, 2014

Scheme 1. (a) Purification Flow for a Protein Complex[a] Eluted from Encapsulated Pea Protein (PP gel) under Aeration and (b) Its Application to the Catalysis (AGPX/CMPX) of Enantioselective Oxidation

a. Process for purification of PX for either AGPX or CMPX.

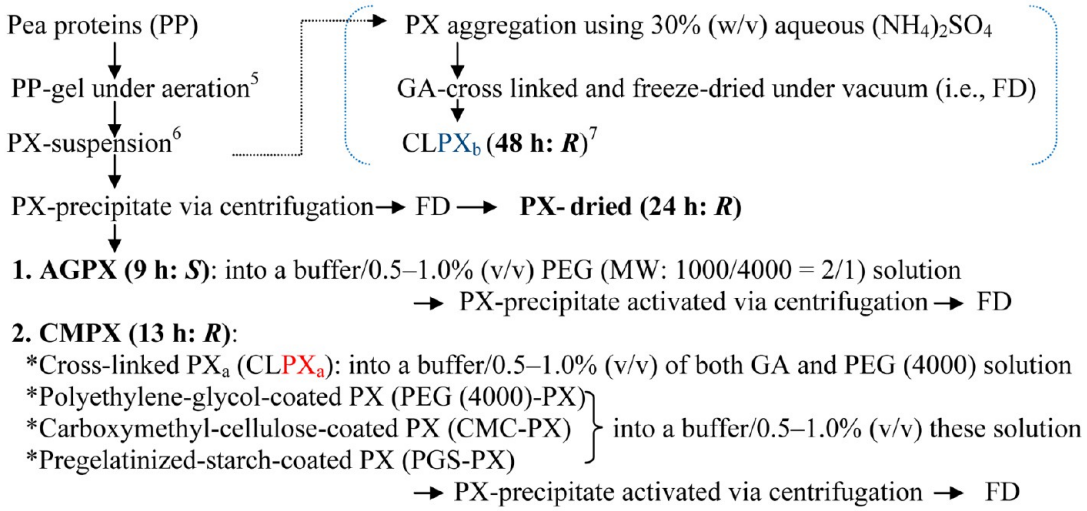

b. Kinetic resolutions of *rac*-**1** and *rac*-**2** using PX-derivatives (AGPX and CMPX).

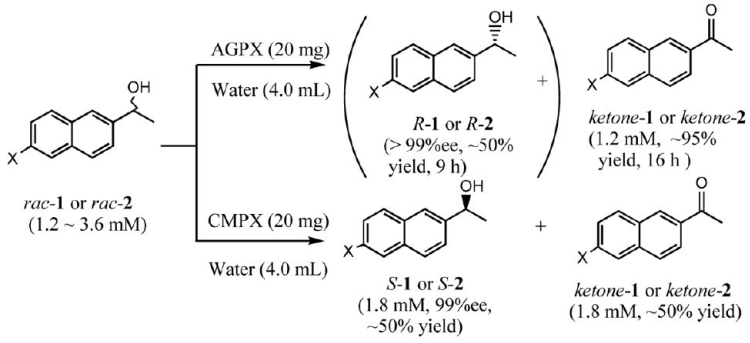

Rac-1: *racemic*-1-(6-methoxynaphthalen-2-yl)ethanol (*S*-naproxen precursor)
Rac-2: *racemic*-1-(2-naphthyl)ethanol
AGPX: PEG(1000)-aggregated PX
CMPX: GA-/compound-modified PX
X: -OCH_3(rac-1), none (rac-2)

[a](PX_a: not treated with $(NH_4)_2SO_4$ or PX_b: treated with $(NH_4)_2SO_4$).

barley leaves, wheat bran, *Artemisia vulgaris* indica, wakame seaweed, carrots, and pumpkins.[6] It has also been shown previously that, in a PX suspension eluted from a PP gel under aeration, PX-redox proteins are both purified and activated by the removal of inhibitors such as metallic cations (Zn^{2+}), chelating agents, and surfactants. That is, a cross-linked PX_b ($CLPX_b$, with $(NH_4)_2SO_4$) was competitively inhibited by 1.0 mM $ZnCl_2$ or a chelating agent (e.g., ethylenediaminetetraacetic acid (EDTA)) or 0.1% (v/v) surfactant (e.g., Tween 20) and further denatured by certain pretreatments (autoclaving at 121 °C (20 min) and adding 6.0 M guanidine−HCl containing 50 mM dithiothreitol).[7]

In particular, it has been shown that, in addition to $CLPX_b$ being particularly activated by a reaction solution of 50 mM glycine−NaOH (pH 9.0−10.0), an iron electron-transfer system may be incorporated as a PX-catalytic system for asymmetric oxidation, with further advantages that neither NAD(P) nor FAD is required for colorimetric analysis and that the oxygen dependency can be observed in a reaction tube without any cap.[7] Therefore, $CLPX_b$ was synthetically applied as a new biocatalyst for the asymmetric synthesis of (*S*)-(+)-1-(6-methoxynaphthalen-2-yl)ethanol (*rac*-**1**: a naproxen precursor,[8] >99% ee) in buffered aqueous media with a cosolvent (DMSO). However, no supporting data characterizing both the initial oxidant and the redox catalytic center have been reported, and the poor activity of a $CLPX_b$ requires improvement to be practically useful in oxidative synthesis with respect to (1) the need for buffered aqueous media and (2) characterization of both the initial oxidant and the redox catalyst center.

In this study, $CLPX_b$ (48 h) was improved, leading to PX_a (a compound-modified PX (CMPX): 13 h), a form that does not contain any trace of $(NH_4)_2SO_4$. A new purification method was developed as follows: the PX precipitate was (1) pretreated in a 50 mM glycine−NaOH solution (pH 9.0−10.0),[7] (2) stored over 20 h after adding 0.5%−1% of a highly polymerized compound (e.g., polyethylene glycol (PEG)), and (3) freeze-dried and crushed. In this case, a PEG (MW: 1000/4000 = 2/

dx.doi.org/10.1021/cs400768x | ACS Catal. 2014, 4, 553−565

Table 1. Elemental Content in the Raw Material Residues from Various PXs Based on the IC Analysis[a]

	IC analysis (wt%)					
sample	C	H	N	S	O	residues
PP	48.83	8.56	12.76	1.78	6.06	——
$CLPX_b$[b]	26.31	7.36	16.09[d]	12.06[d]	23.15[d]	$(NH_4)_2SO_4$
PEG(4000)-PX[c]	46.04	8.34	6.92[e]	1.59[e]	7.85	——

[a]The oxygen content was calculated from the difference in the MW of sulfur (S) and the sulfate anion (SO_4^{2-}). [b]$CLPX_b$ was subjected to "$(NH_4)_2SO_4$" precipitation. [c]PEG (4000)-PX underwent centrifugation and was not subjected to "$(NH_4)_2SO_4$" precipitation. [d]Highest weight percent indicates the reminder of "$(NH_4)_2SO_4$" following the precipitation process. [e]Lowest weight percent indicates that no "$(NH_4)_2SO_4$" remained, but a higher oxygen (O_2) content was detected for the PP.

1)-aggregated PX (AGPX) and a CMPX (either a cross-linked PX ($CLPX_a$) or a highly polymerized-compound-coated PX) is applicable for the kinetic resolution of the turnover: each enantiomer of *rac*-**1** can be selectively synthesized, utilizing PX_a surrounded by a different size molecule (i.e., PEG) (see Scheme 1 for details of the PX purification process and each activity). The specific activity of AGPX/CMPX for oxidative synthesis without an added redox cofactor in water was determined to be 0.8 ± 0.03 mU/0.6 ± 0.02 mU (mean ± SD, where U is unit and 1 U = 1 μmol/(min·mg)). Asymmetric oxidation is attributed to the HBP that eluted from the encapsulated PP, and this conclusion is supported by an N-terminal sequence comparison, which showed a high similarity with the HBP from a PP, a 20.853 kDa hemophore HasA gene product. Therefore, the hemophore itself or its host HBPs may be regenerated by successive asymmetric catalytic events using an incorporated iron electron-transfer system in the presence of oxygen (i.e., $Fe^{2+} + O_2 \rightarrow Fe^{3+}{-}O{-}O^- \rightarrow Fe^{4+}{=}O$ (oxidizing substrate) $\rightarrow Fe^{2+} + H_2O$),[3a−c] a process seemingly similar to that utilized by $P450_{BS\beta}$ or hemoglobin. Thus, these features of this PX-catalytic system incorporating a redox cofactor for asymmetric oxidation are clarified herein.

RESULTS AND DISCUSSION

This study aims to (1) show the improvement in $CLPX_b$ (48 h) that leads to $CLPX_a$ (a CMPX: 13 h), a form not containing any traces of $(NH_4)_2SO_4$; (2) calculate the $CLPX_a$ specific activity (unit/(mg·min)); and (3) characterize the PX initial oxidant and redox catalyst center.

Clarification of CMPX Contents by Physicochemical Verification. *Inductively Coupled Plasma-Atomic Emission Spectroscopy (ICP–AES) Analysis of $CLPX_b$ and the PEG (4000)-PXs.* As shown in Table 1, significant differences were found in the elemental makeup of $CLPX_b$ and PEG (4000)-PX. For example, as compared with PEG (4000)-PX, $CLPX_b$ showed increased levels of N (16.09 wt %), S (11.02 wt %), and O (23.15 wt %), indicating that $(NH_4)_2SO_4$ was retained in $CLPX_b$. In addition, the level of oxygen in PEG (4000)-PX (7.85 wt %) was significantly enriched compared with that in PP (6.06 wt %). It was speculated that oxygen absorption in the PP gel is processed under aeration, which leads to the formation of a reactive oxygen species via an iron electron-transfer system (i.e., cysteine thiolate coordination to iron:[3c] $Fe^{2+} + O_2 \rightarrow Fe^{3+}{-}O{-}O^- \rightarrow Fe^{4+}{=}O$ (+ *rac*-**1**) $\rightarrow Fe^{2+} + H_2O$),[3] resulting in water solubility (PP → PX). This was also supported by the consistency of ML FTIR instrumental analysis because of promoting a reactive oxygen species (cysteine-$Fe^{3+}{-}O{-}O^- \rightarrow Fe^{4+}{=}O$),[4a−c] leading to the appearance of sulfate (SO: e.g., cysteine with oxygen) in the range 950−1250 cm^{-1} (see Supporting Information (SI) Figures S1, S2 and Table S1)[4e].[4] Furthermore, as shown in Figure 1, a comparison of the

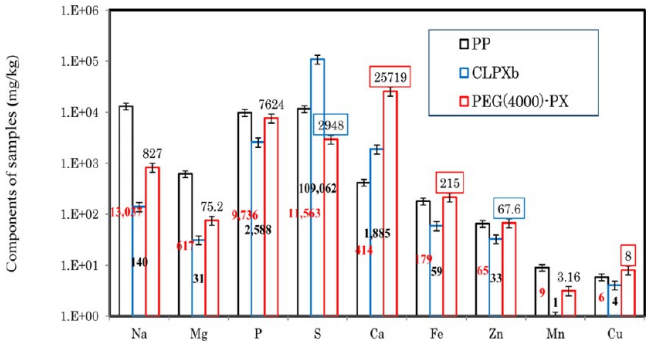

Figure 1. ICP−AES (metal) analysis results: (black) pea protein (PP), (blue) $CLPX_b$ (cross-linked PX treated with 30% (w/v) aqueous $(NH_4)_2SO_4$), and (red) PEG (4000)-PX (not treated with $(NH_4)_2SO_4$).

PEG (4000)-PX (not treated with $(NH_4)_2SO_4$) with $CLPX_b$ showed that the former contained four times the level of iron (215 ppm, PEG (4000)-PX vs 59 ppm, $CLPX_b$), suggesting that the activity of PEG (4000)-PX should be approximately four times as great as that of $CLPX_b$ if an iron electron-transfer system is incorporated (see Table 2 and SI Tables S2−S6). These results indicate that the initial PX-redox oxidant is more active in the presence of a greater proportion of incorporated Fe. Moreover, regarding the ability of the reactant to enter the PX_b surface, over 20% (v/v) of the surrounding $(NH_4)_2SO_4$ may stem from a multisubunit species because of the tendency to dissociate upon dilution, resulting in a longer half-life, albeit with less activity at the start (see SI Figures S1, S2 and Table S1).[7] The results in Figure 1 also show that there were a few differences in the Fe content of PEG (4000)-PX (215 ± 5 ppm) and PP (179 ± 4 ppm) and that no activities were observed. This means that, during the encapsulation of PP under aeration, an incorporated iron electron-transfer system is both purified/concentrated/solubilized and activated by removing the inhibitors present in the aggregates or complexes from the PP, such as metallic cations (Zn^{2+}), chelating agents, and surfactant from PP.[7]

Determination of the Specific Activity of the PXs (unit/(mg·min)). *Differences in the Activity between PX Fractions Separated by Centrifugation and the PX Derivatives.* As shown in Figure 2, the highest asymmetric oxidation activity was observed in the CMC-PX reaction (13 h), and the lowest activities were observed for the $CLPX_b$ reaction (48 h) and PX supernatant reaction (72 h). These results indicate that, although the PX-redox protein is stable to colloid aggregation, similar to highly polymerized systems (e.g., CM-cellulose, PEG (4000), and PG-starch), the PX-active site may be effectively concentrated with the PP-heme during centrifugation (see Table 2), and such a compound-modified

dx.doi.org/10.1021/cs400768x | ACS Catal. 2014, 4, 553−565

Table 2. Catalytic Performance and Mineral Content of Different PXs

		reactions (*rac*-1 or *rac*-2)				minerals[e]	
forms (20 mg)	product	solvent	time (h)	unit[f] (mg·min)	substrate (%)	Ca^{2+} (%)	Fe^{2+} (ppm) (Fe/mol)
$CLPX_b$[a]	(*S*)-1, S-2 ≥ 78% ee, ~50% CY[b]	buffer[d]	48	low	0.02	0.45 ± 0.05	59 ± 2 (≒1 μmol)
$CLPX_a$[a]	(*S*)-1, S-2 ≥ 99% ee, ~50% CY[b]	D.W.[c]	16	0.6 ± 0.02 mU	≥0.06	2.4 ± 0.2	220 ± 5 (≒4 μmol)
PEG (4000)-PX	(*S*)-1, S-2 ≥ 99% ee, ~50% CY[b]	D.W.	14	0.6 ± 0.02 mU	≥0.06	2.6 ± 0.2	215 ± 5 (≒4 μmol)
AGPX	(*R*)-1, R-2 ≥ 99% ee, ~50% CY[b]	D.W.	9	0.8 ± 0.03 mU	≥0.06	2.5 ± 0.2	213 ± 5 (≒4 μmol)

[a]$CLPX_a$ prepared without "$(NH_4)_2SO_4$" precipitation. $CLPX_b$ prepared with "$(NH_4)_2SO_4$" precipitation. [b]Chemical yield (%). [c]Distilled water. [d]50 mM glycine−NaOH (pH 9.0) or 50 mM Tris−HCl (pH 8.0). [e]Mineral values were determined by ICP−AES; mean ± SD (n = 4). [f]Mean ± SD (n = 4).

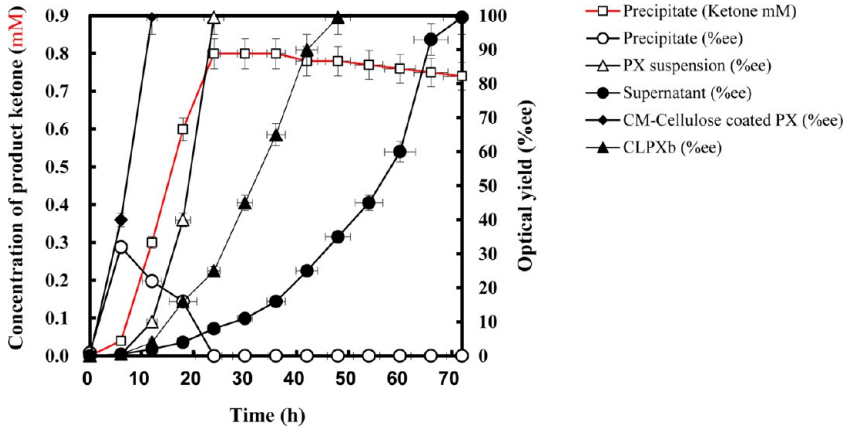

Figure 2. Time course of the asymmetric oxidation activity: (-△-) eluent from the PX suspension of the PP gel (5.0 mL), (-●-) supernatant of the PX suspension acquired via centrifugation (5.0 mL), (-□-, mM; -○-, %ee) aqueous suspension of the sample 1 precipitate acquired via centrifugation (100 mg/5.0 mL D.W.), (-◆-) CM-cellulose-coated PX (20 mg/5.0 mL D.W.), and (-▲-) cross-linked PX_b ($CLPX_b$) treated with 30% (w/v) aqueous $(NH_4)_2SO_4$) (20 mg/5.0 mL 50 mM glycine−NaOH (pH 9.0)). A substrate solution (*rac*-**1**: 20 μL, 20 000 ppm) was then poured into a test tube (18 mm ×15 mL) containing each of the samples prepared above.

treatment may be well justified as a method for improving the activity (i.e., enantioselectivity) and solvent pH independence (i.e., operational stability). Overall, the concentration of the product ketone decreased to <0.6 mM because of its volatility (asymmetric oxidation was performed in a tube without a cap).[7] Thus, the PX suspension, supernatant, precipitate, and CMC-PX may function in the presence of O_2 via a reactive oxygen species (Fe^{2+} + O_2 → Fe^{3+}−O−O^- → Fe^{4+}=O (+ *rac*-**1**) → Fe^{2+} + H_2O).[3a−c] This suggests that the iron-electron-transfer system may lie in the hydrogen peroxide-driven $P450_{BS\beta}$, an HBP that depends on oxygen instead of a redox cofactor (e.g., NAD(P)H).[3a−c] The elemental makeup of the CMPXs and their catalytic performance are summarized in Table 2.

Asymmetric Redox Activity of the CMPXs and $CLPX_a$. Furthermore, using CMPX (20 mg) and *rac*-**1** (1.2 mM), the activity of PEG-PX (MW: 4000) was compared for different concentrations of coating to determine the optimum concentration of PEG (4000), as shown in Figure 3a. The reaction was further examined to determine whether the substrate solution (30 μL, 20 000 ppm) can be added in three portions (0, 8, and 12 h) to the CMPX (20 mg) in 4.0 mL of deionized water (D.W.) without any loss of optical purity or chemical yield, as shown in Figure 3b. During the 30 h of incubation at 40 °C, the substrate concentration (30 μL, 20 000 ppm) increased from 1.2 mM to 3.6 mM, and the aqueous medium decreased from 4.0 mL to nearly 3.5 mL because of volatility (the reaction tube was not capped).[7]

The results for the PX-dried and AGPX CMPXs are summarized in Table 3 and indicated that, when an equimolecular amount of the highly polymerized compound compared with PX is used, the PEG (4000)-PX, CMC-PX, and PGS-PX (20 mg) systems oxidize only the (*R*)-isomer with high enantioselectivity at 13 h; thus, >99% ee of the *S* isomer was obtained from *rac*-**1** (Table 3). In addition, the increase in both the product ketone and unreacted *S* isomer in the aqueous medium was not lost until after three additions (30 h reaction), and the substrate could be added in three portions at 0, 8, and 12 h without any decrease in optical purity or yield. Thus, using CMPX (20 mg in 4.0 mL D.W.), (*S*)-**1** (~1.0 mg, 99% ee) was generated from *rac*-**1** (3.6 mM) in 30 h, as shown in Figure 3b. Furthermore, if no compound modification was applied, no stereoselectivity was observed in the reaction (i.e., non-PEG/freeze-dried (FD): no PEG (4000) and no freeze-drying) with *rac*-**1**, and both isomers were oxidized to the corresponding ketone. These results thus indicated that PX-compound modification improves the intensity or stereoselectivity of asymmetric oxidation in aqueous media, as shown in Figure 3a, and implies that a PX-active site surrounded by 2.6% Ca^{2+} or Ca^{2+} compounds (see Table 2) may affect the ability of the reactant to enter beyond the metallic surface after GA-/highly polymerized compound treatment (see SI Figure S3). In addition, AGPX (treated with PEG (MW: 1000/4000 = 2/1) aggregation) was used for the oxidative conversion of *rac*-**1** to the corresponding ketone (~95% chemical yield: >16 h) via the selective oxidation of (*S*)-(+)-**1**, leaving highly enantiopure (*R*)-(−)-**1** (>99% ee: ~50% chemical yield, <9 h) (see Table 3). Therefore, the turnover of the PX-active site may be affected in the process of PEG (MW: 1000/4000 = 2/1) aggregation such that each enantiomer can be selectively synthesized by utilizing either AGPX (PEG (1000/4000 = 2/1)-aggregated PX) or

dx.doi.org/10.1021/cs400768x | *ACS Catal.* 2014, 4, 553−565

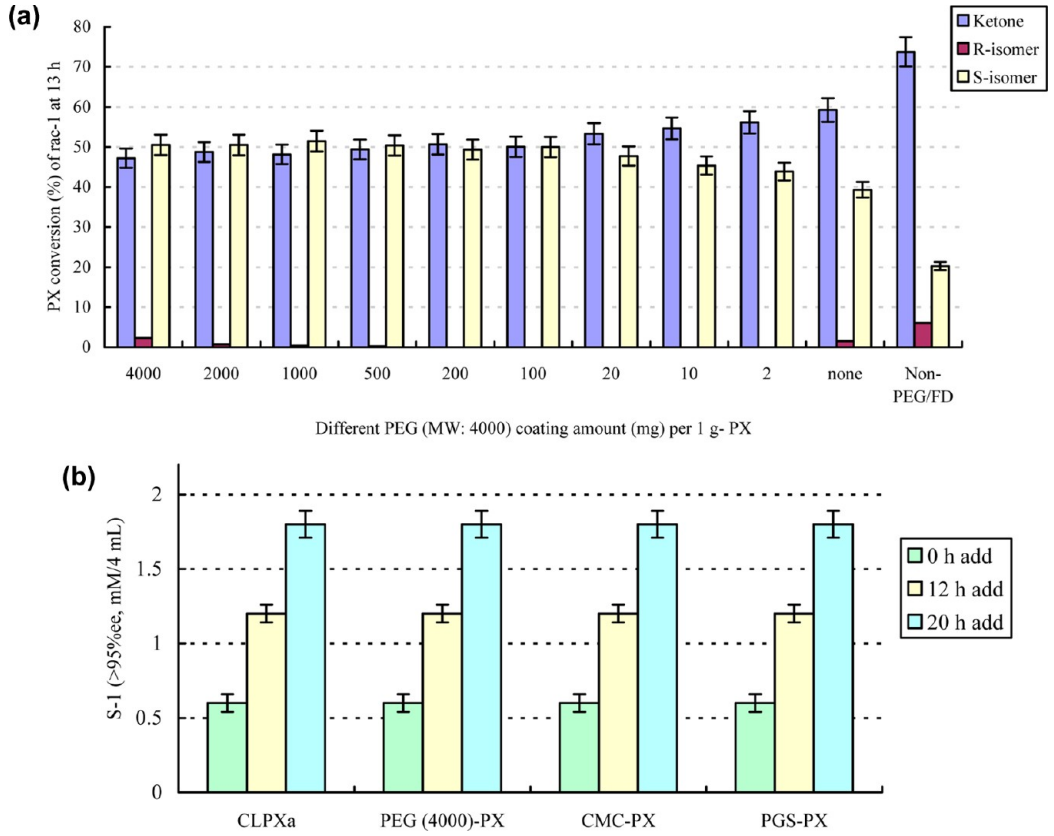

Figure 3. Conversion ratio (%) for the reaction of CMPX (20 mg) with *rac*-**1** (1.2 mM) in distilled water (4.0 mL) and DMSO (0.6% (v/v)) at 40 °C with magnetic stirring at 700 rpm for 13 h: (a) Differences in the amount of PEG (4000) coating (0−4000 mg) on the PX (1 g), (b) 30 h reaction of *rac*-**1** added in three portions at reaction times of 0, 12, and 20 h (1.2 mM × 3).

Table 3. Oxidation Activity of PX Derivatives (PXs) with either *rac*-1 or *rac*-2 (1.2 mM) in the Solvents (4.0 mL)/Cosolvent (< 0.6% (v/v)) at 40 °C

						products	
PXs (20 mg)		times (h)[a]	substrate (1.2 mM)	cosolvent [0.6% (v/v)]	solvent [4.0 mL]	compd	OP/% ee[b]
1	$CLPX_a$	16	rac-**1**	IPA[c]/ DMSO	D.W.[g]	(*S*)-**1**	>99/ >99
		16	*rac*-**2**			(*S*)-**2**	>99/ >99
2	$CLPX_b$	48	*rac*-**1**	IPA/DMSO	D.W	(*S*)-**1**	3.8/5.8
		48	*rac*-**1**		buffer[d]	(*S*)-**1**	79/ >99
		48	*rac*-**2**	IPA/DMSO	D.W.	(*S*)-**2**	2.9/5.2
		48	*rac*-**2**		buffer	(*S*)-**2**	88/ >99
3	PEG (4000)-PX	13	*rac*-**1**	IPA/DMSO	D.W.	(*S*)-**1**	>99/ >99
		13	*rac*-**2**			(*S*)-**2**	>99/ >99
4	CMC-PX	14	*rac*-**1**	IPA/DMSO	D.W.	(*S*)-**1**	>99/ >99
		13	*rac*-**2**			(*S*)-**2**	>99/ >99
5	PGS-PX	14	*rac*-**1**	IPA/DMSO	D.W.	(*S*)-**1**	>99/ >99
		14	*rac*-**2**			(*S*)-**2**	>99/ >99
6	AGPX	9	*rac*-**1**	IPA/DMSO	D.W.	(*R*)-**1**	>99/ >99
		9	*rac*-**2**			(*R*)-**2**	>99/ >99
7	PX-dried[e]	22	*rac*-**1**	IPA/DMSO	D.W.	(*S*)-**1**	>99/ >99
		20	*rac*-**2**			(*S*)-**2**	>99/ >99
						Products	
(20 mg)		times (h)[a]	substrate (1.2 mM)	cosolvent [0.6% (v/v)]	solvent [4.0 mL]	compd	CY %[f]
8	AGPX	16	*rac*-**1**	IPA/DMSO	D.W.	ketone-1	~95/ ~95
		16	*rac*-**2**			ketone-2	~95/ ~95

[a]Reaction time. [b]Optical purity determined by HPLC. [c]2-Propanol. [d]50 mM glycine−NaOH (pH 9.0); $CLPX_a$ is produced without $(NH_4)_2SO_4$; $CLPX_b$ is produced with $(NH_4)_2SO_4$. [e]PX-dried was prepared by freeze-drying after centrifuging the PP gel extract (see Scheme 1). [f]Chemical yield (%). [g]Distilled water.

dx.doi.org/10.1021/cs400768x | *ACS Catal.* 2014, 4, 553−565

CMPX (specifically, $CLPX_a$), as shown in Table 2 (see SI Figure S3 and Table S7).

Determination of the Specific Activity of the CMPXs (unit/(mg·min)). The asymmetric oxidation activity of $CLPX_a$ and AGPX (5, 10, 15, and 20 mg) with *rac*-**1** (1.2 mM) was then determined at 40 °C with magnetic stirring at 700 rpm for 34 h in aqueous media (4.0 mL of D.W.) with water-miscible DMSO (<1.0%). During the 34-h incubation period at 40 °C, the substrate solution (30 μL, 20 000 ppm) was added in three portions at 0, 12, and 20 h. Figure 4a and b shows the

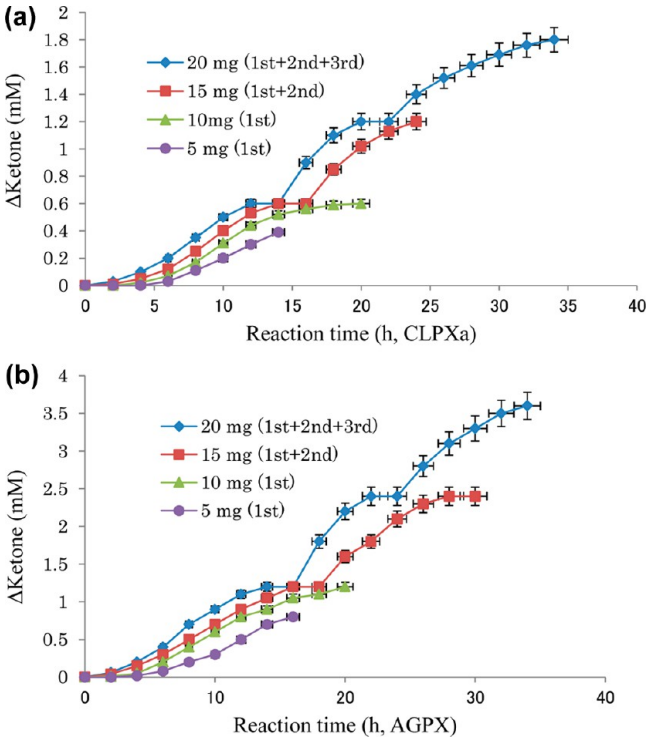

Figure 4. Comparison of the change in ketone concentration (mM) versus time for different quantities of $CLPX_a$ and AGPX in the reaction of *rac*-**1** (1.2 mM × 1−3 portions) in distilled water (4.0 mL) and DMSO (0.6% (v/v)) at 40 °C with magnetic stirring at 700 rpm for 34 h: (a) Asymmetric oxidation activity of $CLPX_a$ (20, 15, 10, and 5 mg) and (b) oxidation activity of AGPX (20, 15, 10, and 5 mg).

dependence of product ketone concentration (mM) on the reaction time (h) for various quantities of $CLPX_a$ and AGPX, respectively, and Figure 5a and b shows the dependence of the instant velocity (mM/h) on the quantity of $CLPX_a$ and AGPX (mg), respectively. The unit indicates that the specified quantity of enzyme is capable of oxidizing 1 μmol of *rac*-**1** per minute.

These results suggest that the activity of $CLPX_a$ is ∼0.6 ± 0.02 mU (mean ± SD)/(mg·min), and the activity of AGPX is ∼0.8 ± 0.03 mU (mean ± SD)/(mg·min), as shown in Figure 5a and b, respectively. The isomer (*S*)-**1** (1.8 mM; 99% ee, ∼50% yield) was obtained from *rac*-**1** (3.6 mM) using $CLPX_a$ (20 mg), and ketone-**1** (3.6 mM; ∼95% yield) was obtained from *rac*-**1** (3.6 mM) using AGPX via the asymmetric oxidation of (*S*)-(+)-**1**, leaving highly enantiopure (*R*)-(−)-**1** (>99% ee: ∼50% chemical yield, 9 h). Overall, the unit of activity for these conversions in comparison with the well-known ADH alternative (100−1000 units) appears to be low; however, the novel aspect of these new biocatalysts is that they do not

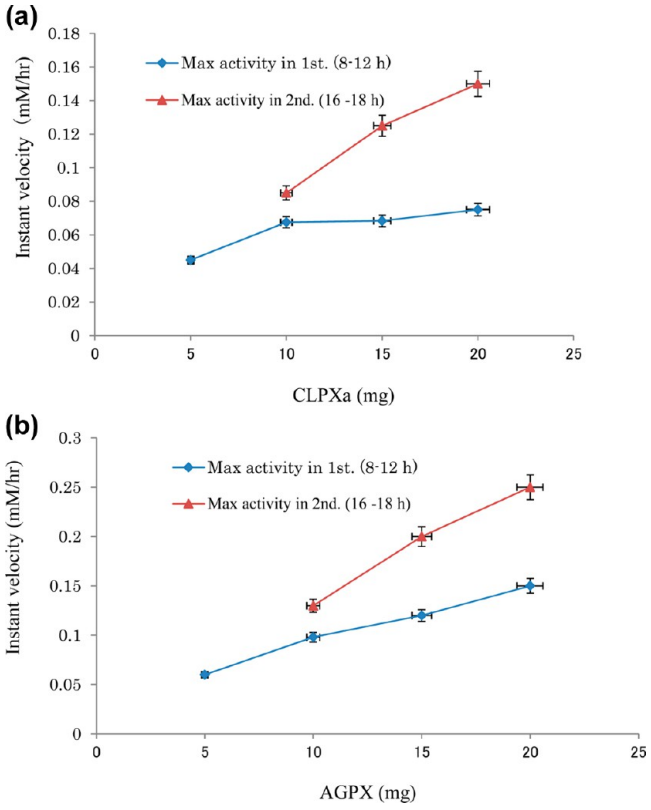

Figure 5. Differences in the specific activity (unit/(mg·min)) of $CLPX_a$ and AGPX: Part a (or b) shows the dependence of instant velocity (mM/h) of $CLPX_a$ (or AGPX) on the quantity of $CLPX_a$ (or AGPX) (mg). This unit indicates the quantity of enzyme (mg) that is capable of oxidizing 1 μmol of *rac*-**1** per minute. The formulas utilized for calculating the instant velocity (IV, mM/h), activity (AC, mmol/(4 mL·min)), and specific activity (SA, unit (mmol/(4 mL·min)) are as follows: IV = Δketone (mM) ÷ time (h), AC = IV (mM/h) × 0.004 (4 mL/L) × 1000 (M/mM) ÷ 60 (min/h), and SA = AC (mol/(4 mL·min)) ÷ $CLPX_a$ (or AGPX) (mg).

depend on the redox cofactor NAD(P), but on oxygen.[7] Thus, the difficulties of working with a pure dehydrogenase enzyme/redox cofactor system has been shown to be surmountable (see SI Table S7).

Sodium Dodecyl Sulfate−Polyacrylamide Gel Electrophoresis (SDS−PAGE) of the PX-Redox Protein for MW Determination. To determine the nature of the PX-redox protein that catalyzes asymmetric oxidation, the PX suspension (10 mL) eluted from the PP gel, which was incubated for 48 h, was first separated into 60 fractions (acquired in 18 mm test tubes with 3.0 mL portions in each tube) using a gel-filtration system, and the absorbance was monitored at 280 nm (see SI Figures S4−S6). These 60 fractions (3.0 mL portions) were each added to 0.48 mL of an aqueous solution of *rac*-**2** (0.8 mM) containing 1.03% (v/v) DMSO. The resulting mixtures were then incubated at 40 °C for 48 h with magnetic stirring at 700 rpm (see SI Figure S7) and subjected to SDS−PAGE analysis. The results of the analysis were compared with those for sample **F** (an aqueous solution containing the gel-filtered PX-redox protein (fraction 36)), and it was determined that the PX-redox protein molecular mass is ∼20 kDa, measured as a single band (PX-redox protein band), corresponding to the respective marker, as shown in Figure 6 (see SI Tables S9 and S10).

dx.doi.org/10.1021/cs400768x | ACS Catal. 2014, 4, 553−565

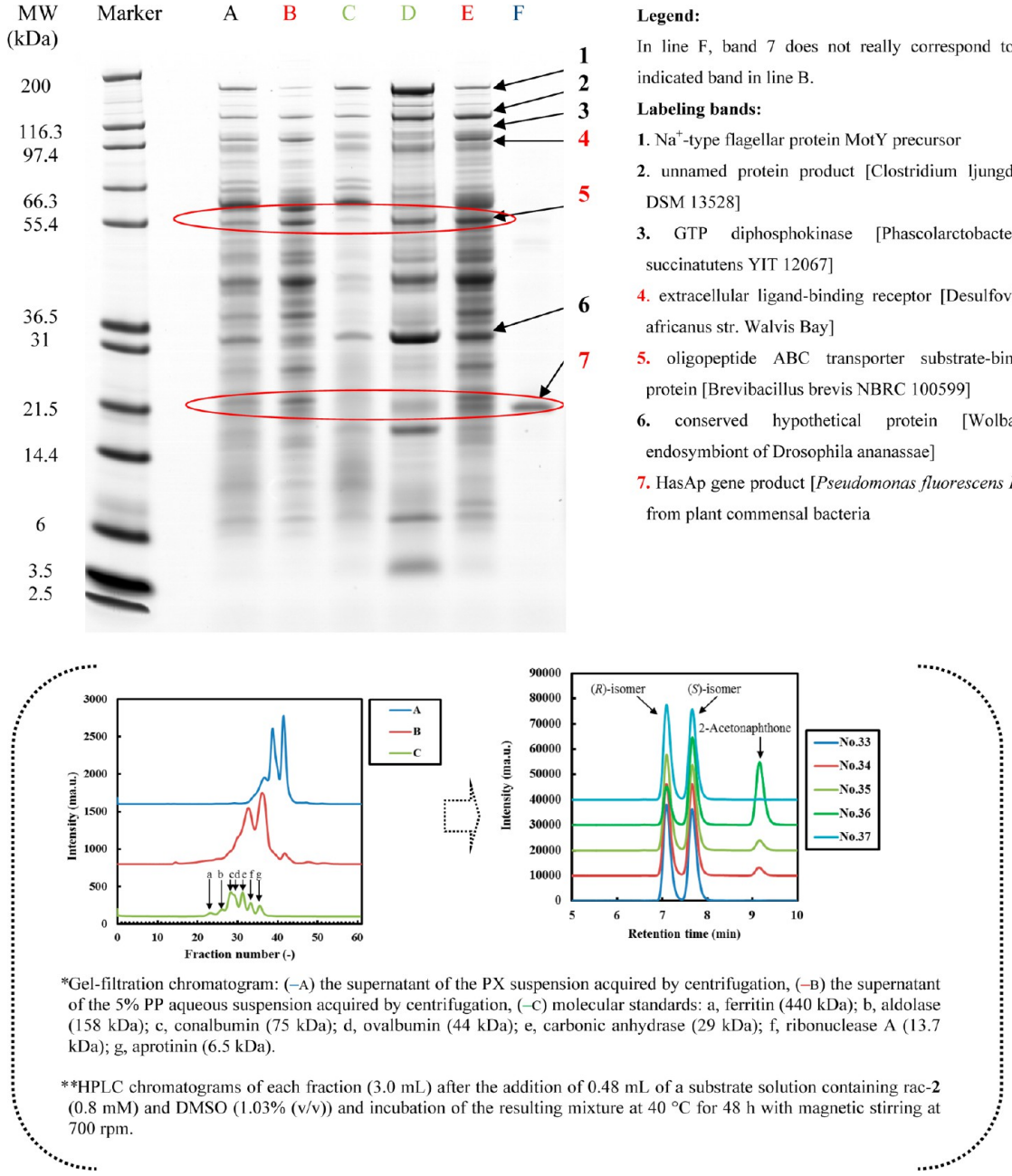

Figure 6. SDS−PAGE of six samples. (A) Eluant from the PX suspension of the PP gel (10 μL), (B) aqueous suspension of the sample A precipitate acquired via centrifugation (10 μL), (C) sample A supernatant acquired via centrifugation (10 μL), (D) aqueous suspension acquired via the centrifugation of the sample C precipitate generated using 30% (w/v) saturated $(NH_4)_2SO_4$ (10 μL), (E) aqueous suspension acquired via the centrifugation of the sample A precipitate generated using 30% (w/v) saturated $(NH_4)_2SO_4$ (10 μL), and (F) fraction 36 obtained via gel-filtration chromatography using a HITEC-CR20G (Hitachi) system at 10 000 rpm (10 min).

These results indicated that when the suspension (10 mL) is directly injected onto the column, gel-filtration alone can provide a single band for **F**. In addition, it was found that different concentrations of sample **F** (PX-redox protein), sample **A**, and sample **B** (**A** and **B** are the suspensions for producing $CLPX_a$) had to be evaluated for the PX-redox protein concentration; therefore, their concentrations were determined by the Bradford method (see SI Table S8). This result also indicated that ∼5%− 7% of the PX-redox protein is present per CMPX. The results of both peptide mass fingerprinting (PMF) and liquid chromatography/mass spectrometry-ion trap-time-of-flight (LC/MS-IT-TOF) analyses indicated that the remaining components (>90%) of CMPX (i.e., the labeled bold bands 1−6) consist mainly of debris from the damaged cell membranes and cell walls of PP, such as an extracellular ligand-binding receptor (band 4) and oligopeptide ABC transporter substrate-binding protein (band 5), as shown in Figure 6 (see SI Tables S9 and S10). These results therefore confirm that hemophore HasA (band 7) is secreted by the ABC transporter (band 5) that exists in the extracellular matrix and/or outer membrane (band 4) of PP.[4a] Furthermore, as previously reported, the ABC transporters appear to have a molecular weight greater than that of the hemophore,[4c] (i.e., band 5/band 7 = approximately 55.4 kDa/20.8 kDa).

dx.doi.org/10.1021/cs400768x | ACS Catal. 2014, 4, 553−565

Table 4. Results of a BLAST Query Sequence Analysis[19] Based on the N-Terminal Amino Acid Sequence Identified from Fraction 36 (band 7)

Cycle No. for fraction 36 (band 7)
N-terminal amino-acid sequence identified (33 residues)

1. X^aSX^{a}SISYSTX^b YATNTVAQYL X^{a}DWX^{b}AYFGDL NHRE

Cycle No. for YP 262445.1[c]
Protein sequence based on a BLAST query sequence analysis[19]

1. MSISISYSAT YGGNTVAGYL TDWSAYFGDV NHRPGEVVDG TNTGGFNPGP
50. FDGTQYAIKS TASDAAFVAD GNLHYTLFSN PSHTLWGSVD TISLGDTLAG
100. GSGSNYNLVS QEVSFTNLGL NSLKEEGRAG EVHKVVYGLM SGDSSALAGE
150. IDALLKAIDP SLSVNSTFDD LAAAGVAHVN PAAAAAADVG LVGVQDVAQD
200. WALAA

Full length gene sequences for hemophore [c]YP 262445.1[19]

atgagcatttcgatctcttacagcgctacctacggcggtaatactgttgcgcaatacctgactgactggtcggcctacttcggcgacgtcaaccaccgcc
caggcgaagtggtcgacggcaccaacaccggtggcttcaacccgggcccgttcgacggcacccagtacgccatcaagagcaccgccagtgacgc
ggccttcgtcgccgacggcaacctgcactacaccctgttcagcaacccgagccacaccctgtggggctcggtggacactatctccctgggcgacacc
ctcgccggtggttcgggcagcaactacaacctggtcagccaggaagtcagcttcaccaacctgggcctcaacagcctgaaggaagaaggccgtgca
ggcgaagtgcacaaggtggtctacggcctgatgagtggcgacagctcggcgctggccggcgagatcgatgccctgctcaaggcgatcgacccaag
cctgtcggtgaactccaccttcgacgacctggccgctgctggcgttgctcacgtcaacccggctgccgcagccgctgccgatgttggcctggtgggtgt
gcaggacgtggcccaggactgggcgctggccgcctga

X^a: may be Cys (C) but not detected, X^b: many amino acids were detected.
[c]YP 262445.1: The accession hit on the query sequence was limited between the query coverage (>93%) and E value (2e-11), a 20.853 Da HasAp gene product [hemophore: *P. fluorescens Pf-5*] from plant commensal bacteria, which can inhibit the rhizosphere and produce secondary metabolites that suppress soil-borne plant pathogens.[9]
Red amino acids indicate "hits" between fraction 36 and YP 262445.1[c].
Squares indicate the heme-binding site: His-32 (bearing loop), Tyr-75 (axial heme ligand), and His-83 (hydrogen ligand).

Identification of the PX-Redox Oxidant via Physicochemical Analysis. *N-Terminal Amino Acid Sequence/Basic Local Alignment Search Tool (BLAST) and PMF and LC/MS-IT-TOF/MASCOT Analysis.* As shown in Table 4, the amino acid sequence (33 residues) of the PX-redox protein band (band 7) was detected, and an N-terminal sequence comparison showed 93% similarity with the HBP, a 20.853 kDa HasAp gene product [*Pseudomonas fluorescens Pf-5*, a plant commensal bacterium], and a similar E value (2×10^{-11}). The molecular mass of the PX-redox protein (equivalent to the HBP) was equal to that obtained from the SDS−PAGE result (20 kDa). Furthermore, at the molecular level of studies in *Serratia marcescence* homophore HasA (see Scheme 2b), it was indicated that the PX-redox protein is a hemophore HasA (heme acquisition system, Has), because the heme ion is bound by axial coordination with His-32 (bearing loop), Tyr-75 (axial heme ligand), and His-83 (hydrogen bound), which reside in opposing loops at the edge.[4b] This is acceptable consistently in both Table 4 and Scheme 2. Thus, although no BLAST-hit data exemplifying a hemophore HasA gene was detected from the plant, as shown in Table 4 for the connection between HBP (*P. fluorescens Pf-5*) and PP, it is thought that the existence of the hemophore may be due to broad acquisition by the plant (e.g., PP), rather than by bacterial contamination.[4b] This conclusion is supported by the consistency of both the part of the pea plant that was utilized (i.e., the PP originated not from the rhizosphere, but from the bean therein) and the germ-free process used for PX purification (see Scheme 1).[5]

Reference 9 indicates that *P. fluorescens Pf-5* is a rhizosphere inhabitant that is resistant to the toxic effect of antibiotics. As direct evidence of PP-heme, there are also several reports demonstrating that hemophore HasA are secreted by living organisms (e.g., plants and bacteria).[4b] For example, *P. fluorescens* varieties have diverse high-affinity heme uptake systems for the various heme sources that they might encounter (such as hemoglobin, hemopexin, and myoglobin).[10] One such system is dependent on "hemophores" that bind heme with high affinity and fulfill a function similar to that of siderophores.[11] These hemophores are also secreted into the extracellular matrix, where they scavenge free or protein-bound heme and then deliver it to a specific cell surface receptor (see Scheme 2);[12] that is, the heme intake system consists of HasA (heme acceptor) ∼ HasR (hemo-receptor) ∼ heme.[13] Thus, the system is not dependent on the redox cofactor (e.g.,

dx.doi.org/10.1021/cs400768x | ACS Catal. 2014, 4, 553−565

Scheme 2. (a) Cell Membrane Protein Containing a Pyrroloquinoline Quinone ADH (PQQ-ADH)[17] with Incorporated Cyt*c*O Characteristics[18] and (b) Crystal Structures of the Outer Membrane Receptor[a] and Excreted Heme-Binding Proteins[b,c]

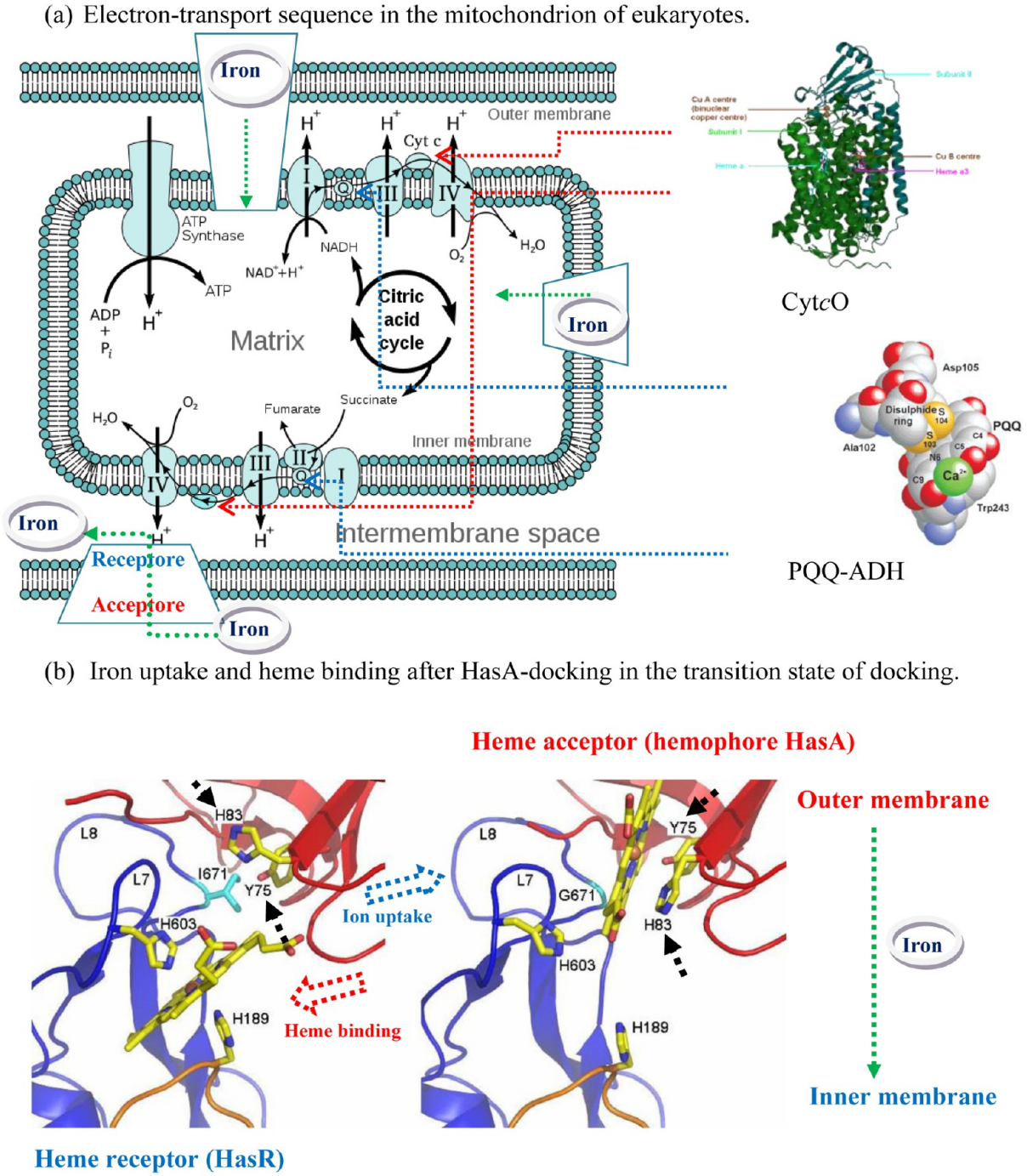

[a]HasR in blue. [b]Hemophore HasA in red. [c]The *Serratia marcescence* homophore HasA, a 188-redidue protein, is bound by axial coordination with HasA-His-32 (bearing loop), HasA-Tyr-75 (axial heme ligand), and HasA-His-83 (hydrogen ligand).[4b]

NAD(P)), but instead on oxygen, and it is thought that the reduced iron (Fe^{2+}: cysteine thiolate coordination to iron) is soluble but highly toxic as a result of the promotion of the formation of a reactive oxygen species (Fe^{3+}–O–O^{-} → Fe^{4+}=O) because of promoting an O_2 driven iron electron-transfer system.[3a−c,14]

In addition to the hemophore HasA of living organisms, it has also been reported that the membrane-bound enzymes of HBPs (e.g., plant-HBPs or bacterial-HBPs) produce secondary metabolites that enable the detoxification of many organic compounds as energy sources and are resistant to the toxic effects of antibiotics.[9] For example, cytochrome-P450s, the pea plant (*Pisum sativum*), and the soil bacterium BM-3 (*Bacillus megaterium*) catalyze the α-hydroxylation of carboxylic acids in the presence of oxygen in aqueous media.[15]

In addition, there are several reports describing membrane-bound enzymes of HBPs with incorporated iron, such as (1) peroxidase,[16] (2) pyrroloquinoline quinone ADH (PQQ-

dx.doi.org/10.1021/cs400768x | ACS Catal. 2014, 4, 553−565

ADH),[17] and (3) CytcO.[18] The oxidation reactions revealed in these studies[16−18] demonstrate (1) peroxide dependence, (2) primary alcohol dependence, and (3) oxygen independence, respectively. Obviously, the peroxidase process (H_2O_2 + HBP − H_2 → $2H_2O$ + HBP) is not comparable to HBP oxidation due to peroxide dependence. Therefore, the regeneration system for HBP can be considered similar in nature to that of (2) primary-alcohol-dependent ADH (PQQ-ADH; namely, CC_1) with incorporated (3) cytochrome *c* oxidase characteristics (namely, CC_2). This system is depicted as follows: (2) $4Fe^{2+} - CC_1 + 8H^+_{in} + O_2 \rightarrow 4Fe^{3+} - CC_1 + 2H_2O + 4H^+_{out}$ in conjunction with (3) $2Fe^{2+} - CC_2 \rightleftarrows$ ketones $+2Fe^{3+}$ − reduced-CC_2 (existing in the cell membrane protein, see Scheme 2). It is supposed that, because the sequence of hemophore HasA is an axis (i.e, bone) secreted by the HBP host proteins (e.g., ABC transporters, PQQ-ADH, and CytcO), the PP-HBP (the hemophore itself and/or its host HBPs) with the incorporated iron-electron-transfer system may be enabled in the presence of oxygen (i.e., $Fe^{2+} + O_2 \rightarrow Fe^{3+}-O-O^- \rightarrow Fe^{4+}=O$ (oxidizing *rac*-**1** or *rac*-**2**) → $Fe^{2+} + H_2O$),[3a−c] which is observed when the O_2 concentration is varied, as a hydrogen peroxide-driven PP-HBP that depends on oxygen instead of a redox cofactor (e.g., NAD(P)H).[3a−c,14] Thus, the reason why these new biocatalysts do not depend on a redox cofactor (e.g., NAD(P)) but instead on oxygen may be clarified here,[7] although there are no supporting studies specifically related to systems for the asymmetric oxidation of secondary alcohols in organic synthesis.[3,4]

The equations indicate that the HBP-redox catalytic center (i.e., the hemophore itself or its host HBPs) can be regenerated for successive catalytic events only in the presence of O_2 and the incorporated O_2-driven cysteine thiolate coordination to the iron-electron-transfer system ($Fe^{2+} \rightleftarrows Fe^{3+}$ with O_2). Further explorations of the full-length gene sequence of the PP-HasA homologue and of the cloning for study of its molecular levels are being actively pursued in this laboratory, and the results will be reported in due course (see Table 4). The novel aspects of these results include not only a new method for the purification and characterization of the compound-modified HBP system and a proposal for the HBP pathway but also the use of a raw biomaterial as a PX-catalytic system incorporating a redox cofactor to perform asymmetric oxidation.

CONCLUSION

This study aimed to clarify the exact nature of all of the species engaged in the biocatalytic oxidation sequence, including that of the PX eluted from encapsulated PP under aeration in both its PEG (MW: 1000/4000 = 2/1)-aggregated PX (AGPX) and compound-modified form (CMPX). The AGPX complex represents a new biocatalyst enabling the oxidation of *rac*-(+)-1-(6-methoxynaphthalen-2-yl)ethanol (*rac*-**1**) to the corresponding ketone-**1** (∼95% yield) via the asymmetric oxidation of (*S*)-(+)-**1**, leaving highly enantiopure (*R*)-(−)-**1** (>99% ee, ∼50% chemical yield). Further, CMPX enables the kinetic resolution of (*S*)-(+)-**1** (an (*S*)-(+)-naproxen precursor; >99% ee, ∼50% yield) via the selective oxidation of (*R*)-(−)-**1** in aqueous media. The activities of both AGPX and CMPX were found to be 0.8 ± 0.03 mU (mean ± SD)/(mg·min) and 0.6 ± 0.02 mU (mean ± SD)/(mg·min), respectively. The asymmetric oxidation activity is attributed to an HBP that is native to the pea plant. The N-terminal sequence comparison showed 93% similarity with the 20.853 kDa HasAp gene product [hemophore HasA, *P. fluorescens Pf-5*] HBP. The PP-HBP (the hemophore itself or its host HBPs) performs successive asymmetric catalytic events (i.e., regeneration) via an incorporated iron electron-transfer system ($Fe^{2+} \rightleftarrows Fe^{3+}$) in the presence of oxygen (O_2). Our findings open up new possibilities for the use of these materials not only as food but also as biological catalysts for the synthesis of optically active alcohols in an environmentally friendly manner, thereby promoting industrial sustainability.

MATERIALS AND METHODS

Preparation of $CLPX_a$, $CLPX_b$, and AGPX. PP (10 g) was added to 200 mL of 0.75% aq. sodium alginate and encapsulated with $CaCl_2$ (500 mL, 39 g/L). The PP gel was then exposed to air for 5 h, and the resulting PX suspension was extracted at 40 °C with distilled water (200 mL) in a 500 mL Erlenmeyer flask with rotary shaking at 150 rpm for over 40 h. For AGPX production, the PX precipitate (wet: 16 g) was centrifuged (15000*g* for 10 min) and then dissolved in a 0.5%−1.0% (v/v) PEG (MW: 1000/4000 = 2/1)/50 mM glycine−NaOH solution (pH 9.0, 100 mL) and stored for over 20 h to allow aggregation, After centrifugation, the precipitate was freeze-dried under vacuum and crushed using a ball mill. For $CLPX_a$ production, the PX-precipitate (wet: 16 g) was dissolved in a 50 mM glycine−NaOH solution (pH 9.0, 100 mL), and then a 25% (v/v) aqueous GA solution (2 mL) was added to obtain an overall 0.5% (v/v) GA solution for cross-linking, which was allowed to take place for over 20 h. After centrifuging the mixture (15000*g* for 10 min), the resulting precipitate was freeze-dried under vacuum and crushed using a ball mill. For $CLPX_b$ production, the PX solution (200 mL), precipitated using 30% (w/v) aq. $(NH_4)_2SO_4$, was cross-linked at 0.25% (v/v) GA via the addition of a 25% (v/v) aq. GA solution (2.0 mL), and the resulting mixture was stored for over 20 h. After centrifuging the mixture (15000*g* for 10 min), the resulting precipitate was freeze-dried under vacuum and then crushed using a ball mill. An RLE-II 203 instrument was utilized to freeze-dry the samples under vacuum [−50 °C/10 Pa (1 h) → 5 °C/min → +50 °C/10 Pa (22 h)].

Preparation of PEG (4000)-PX, CMC-PX, and PGS-PX. The protocol for the purification/preparation of PEG (4000)-PX, CMC-PX, and PGS-PX is as follows: (1) formation of the PP gel by the encapsulation of the PP (10 g) with a calcium alginate gel prepared from a 0.75% aq. sodium alginate solution (200 mL D.W.) and a 39 g/L $CaCl_2$ solution (500 mL) (PP gel); (2) aeration of the PP gel in air for several hours; (3) extraction of the contents by rotary shaking using hot water to obtain a PX suspension; (4) separation of the precipitate from the suspension by centrifugation (15000*g*, 10 min); (5) coating the precipitate (wet: 5.0 g) via the addition of PEG (MW, 4000), CM-cellulose, or pregelatinized starch (500 mg) dissolved in 50 mM glycine−NaOH (pH 9.0) buffer (50 mL); and (6) preparation of the coated powder (∼1.0 g) via freeze-drying and crushing using a ball mill. The CMPCs were optionally prepared using different relative amounts of PEG (4000), CM-cellulose, or pregelatinized starch (∼2.0 g, 1.0 g, 500 mg, 250 mg, and 125 mg per 1.0 g of dried PX) dissolved in distilled water (500 mL). An RLE-II 203 instrument was utilized for freeze-drying of the samples under vacuum [−50 °C/10 Pa (1 h) → 5 °C/min → +50 °C/10 Pa (22 h)]. To confirm the presence of the PX-redox protein that catalyzes the asymmetric oxidation of secondary alcohols, a portion of the PX suspension eluted from the PP gel was separated into two fractions via centrifugation (15000*g*, 10 min): the supernatant

dx.doi.org/10.1021/cs400768x | ACS Catal. 2014, 4, 553−565

and precipitate. The precipitate (5.0 g) was dissolved in a 50 mM glycine−NaOH (pH 9.0) buffer (50 mL), and a portion of this solution was coated with CM-cellulose (500 mg) to produce CMC-PX (1 g). Next, a substrate solution (30 μL, 20 000 ppm) was added to test tubes (18 mm ×15 mL) containing each of the samples prepared above: the PX suspension (5.0 mL), the supernatant (5.0 mL), the aqueous solution of the precipitate (100 mg/5.0 mL D.W.), and the CMC-PX aqueous solution (20 mg/4.0 mL D.W.). The reactions were performed at 40 °C with magnetic stirring at 700 rpm, and the results are shown in Figure 2.

Confirmation of the Composition of PEG (4000)-PX, CLPX, and PP. To determine if certain raw materials, such as $(NH_4)_2SO_4$ and sodium/calcium alginate, were retained in the CMPCs, the difference in the elemental makeup of $CLPX_b$ and PEG (4000)-PX was examined. The content of $(NH_4)_2SO_4$ and sodium/calcium alginate was determined by the following methods. Measurement of the metal content was conducted by adding the protein powder (0.5 g) to a solution of purified water (50 mL) and 60% HNO_3 (Kokusan, 10 mL) in a 100 mL beaker, followed by the digestion of the resulting mixture (heating on a hot plate for 1 h). The digested sample was diluted to 50 mL with purified water, and the metal content was measured by inductively coupled plasma−atomic emission spectrometry (ICP−AES; Shimadzu, ICPS-7500). Elemental analysis of the samples (2 mg) was performed on a Perkin-Elmer PE 2400 Series II analyzer.

Determination of the Specific Activity of the CMPXs and AGPX in Biocatalytic Reactions. *General Procedure for the Reactions Using the CMPXs and AGPX.* *rac*-**1** (1000 mg) was dissolved in DMSO as a cosolvent (50 mL). The substrate solution (30 μL, 20 000 ppm) and CMPX (20 mg) were combined in an 18 mm ×15 mL test tube in distilled water (4.0 mL), and the reactions were performed at 40 °C with magnetic stirring at 700 rpm. Subsequently, the reaction mixture was centrifuged at 2000*g* (5 min) and then extracted by adding *n*-hexane (4.0 mL). The ee was calculated for either *rac*-**1** (0.8 mM or 1.2 mM) or *rac*-**2** (0.8 mM or 1.2 mM), which were separated using either a Daicel Chiralcel OB-H column (*S* isomer/*R* isomer/product ketone = 7.8/8.8/11.6 min) or a Daicel Chiralpak AS-H column (*S* isomer/*R* isomer/product ketone = 7.5/8.25/9.5 min) connected to an HPLC LC-10A system (Shimadzu). The analytical conditions were as follows: mobile phase, *n*-hexane/IPA, 9/1; flow rate, 1.0 mL/min; temperature, 30 °C; wavelength, UV 254 nm. The stereochemistry of the isolated optically active alcohol was identified as reported previously[5] by comparing the specific rotation values (+ or −) obtained using a polarimeter.

Determination of the Specific Activity (unit/(mg·min)) of the CMPXs and AGPX. The asymmetric oxidation activity of $CLPX_a$ (5, 10, 15, and 20 mg) and the oxidation activity of AGPX (5, 10, 15, and 20 mg) with *rac*-**1** (1.2 mM) in water (4.0 mL D.W.) and DMSO (<1.0%) with magnetic stirring (700 rpm) for 34 h was measured. During the 34 h incubation period at 40 °C, the substrate solution (30 μL, 20 000 ppm) was added in three portions at 0, 12, and 20 h. Figure 4 shows the dependence of the concentration of the product ketone (Δketone: mM) on the reaction time (h) for different quantities of $CLPX_a$ (or AGPX). Figure 5 shows the dependence of the instant velocity (mM/h) of $CLPX_a$ (or AGPX) on the quantity of $CLPX_a$ (or AGPX) (mg). This unit indicates the quantity of enzyme (mg) that is capable of oxidizing 1 μmol of *rac*-**1** per minute. The formulas utilized for calculating the instant velocity (IV, mM/h), activity (AC, mmol/(4 mL·min)), and the specific activity (SA, unit (mmol/(4 mL·min)) are as follows: IV = Δketone (mM) ÷ time (h), AC = IV (mM/h) × 0.004 (4 mL/L) × 1000 (M/mM) ÷ 60 (min/h), and SA = AC (mol/(4 mL·min)) ÷ $CLPX_a$ (or AGPX) (mg).

Separation of the PX-Redox Protein from the Suspension. *Gel-Filtration Chromatography of the Suspensions Eluted from the PP Gel.* The PX suspensions eluted from the PP gel using water at 40 °C were subjected to gel filtration to produce the following samples: (A) supernatant of the PX suspension obtained via centrifugation, (B) supernatant of a 5% PP aqueous suspension obtained via centrifugation, and (C) molecular standards: a, ferritin (440 kDa); b, aldolase (158 kDa); c, conalbumin (75 kDa); d, ovalbumin (44 kDa); e, carbonic anhydrase (29 kDa); f, ribonuclease A (13.7 kDa); and g, aprotinin (6.5 kDa). Each sample (10 mL) was injected onto a HiLoad16/60 Superdex 200 pg column at 4 °C equilibrated with Tris−HCl (50 mM) and NaCl (150 mM, pH 8.0). The column was connected to a KTA explorer 10S system. The column flow rate was maintained at 0.5 mL/min, and the absorbance was monitored at 280 nm. The fractions (3.0 mL) obtained by gel filtration were used for the asymmetric oxidation of *rac*-**1** with 1.03% (v/v) DMSO in an 18-mm test tube at 40 °C, which was facilitated by stirring at 700 rpm for 48 h (total volume of 3.48 mL). After extraction by the addition of 3.0 mL of *n*-hexane, the fractions were subjected to HPLC chromatography using an LC-10A (Shimadzu) column.

SDS−PAGE of the PX Suspension Eluted from the PP Gel. SDS−PAGE was performed on the following samples: (A) eluant of the PX suspension from the PP gel (10 μL), (B) aqueous suspension of the precipitates from sample A obtained by centrifugation (10 μL), (C) supernatant from sample A obtained by centrifugation (10 μL), (D) aqueous suspension of the precipitates from sample C obtained by centrifugation after treatment with 30% (w/v) saturated $(NH_4)_2SO_4$ (10 μL), and (E) aqueous suspension of the precipitates from sample C obtained by centrifugation at 12 000 rpm using a HITEC-CR20G (Hitachi) system (20 min) after treatment with 30% (w/v) saturated $(NH_4)_2SO_4$ (10 μL). Sample F was an aqueous solution containing the gel-filtered PX-redox protein (fraction 36). Each sample (10 μL) was heated at 100 °C (5 min) after mixing with 2× SDS sample buffer (Sigma-Aldrich) and electrophoresing with a molecular marker (Biorad) in a buffer (Tris−HCl (25 mM) and glycine (0.91 M), 0.1% SDS, pH 8.3) using an SDS−PAGE mini system (TEFCO). After completion, the gel was stained with CBB (PhastGel Blue R, Amersham Bioscience).

Identification of the PX-Redox Proteins by Physicochemical Analysis. *N-Terminal Amino Acid Sequence and BLAST Analysis of Fraction* ***36****.* Precise analysis of the N-terminal amino acid sequence (protein sequencing) of the single band 7 of the PX-redox protein in sample F obtained via SDS−PAGE was accomplished using the PPSQ-21A protein sequencer (Shimadzu). This method excises the amino acids one by one from the N-terminus of the protein or peptide (Edman degradation method). Separation by HPLC with UV detection enabled the determination of the amino acid sequence from the peak retention times (chromatograms). Blotting was achieved at a constant voltage (25 V) for 1 h using a Fluorotrans membrane (Pall), NuPAGE transfer buffer (Invitrogen), CBB-R250 (BIO-RAD), and 50% methanol with 5% acetic acid. The targeted band of the polyvinylidene

dx.doi.org/10.1021/cs400768x | ACS Catal. 2014, 4, 553−565

difluoride membrane near 20 kDa was also measured to determine the amino acid sequence using the protein sequencer PPSQ-21A (Shimadzu). The obtained amino acid sequence was acquired using BLAST to identify regions of local similarity between the sequences.

PMF, LC/MS-IT-TOF, and MASCOT Analysis of the SDS Bands. In-gel digestion of the other six obtained bands (single bands 1−6 via SDS−PAGE) was performed as follows: After each band was incubated in a buffer (500 μL; guanidine (7 M), Tris−HCl (0.5 M, pH 8.5), and EDTA (10 mM)), alkylation was performed by the addition of β-mercaptoethanol (2 μL), 4-vinylpyridine (2 μL), and 0.1% TFA (500 μL). The gels were washed with 20 mM ammonium bicarbonate followed by neat acetonitrile, and then Lys-C (10 μL, 0.01 mg/mL) was added, and the peptide-containing gels were subsequently extracted using 0.1% TFA/50% aq. acetonitrile and neat acetonitrile. The peptide extracts were concentrated to 10 μL on an evaporator and were then demineralized using Ziptip μC-18 columns (Millipore). The peptide mixtures were analyzed by mass spectrometry using the following instruments and conditions: (1) LC/MS-IT-TOF (Shimadzu: mode, nanoESI$^+$; MS range, MS1 (m/z 400−1500) and MS^2 (m/z 50−1500) data-dependent scan; flow rate, 300 nL/min; flow solvents, A = 0.1% formic acid/2% acetonitrile, B = 0.1% formic acid/80% acetonitrile; gradient, 5−40% B/0−30 min, 40−100% B/30−40 min, 100% B/40−60 min) and (2) BIFLEX III (Bruker Daltonics: mode, positive/reflector; matrix, α-cyano-4-hydroxy cinnamic acid (CHCA); target plate; and peptide calibration standards: angiotensin II ($[M + H]^+$ = 1046.542), angiotensin I ($[M + H]^+$ = 1296.685), substance ($[M + H]^+$ = 1347.736), bombesin ($[M + H]^+$ = 1619.823), ACTH1−17 ($[M + H]^+$ = 2093.087), ACTH18−39 ($[M + H]^+$ = 2465.199)). MASCOT analysis based on the peak lists obtained by mass spectrometry was performed as follows: database, National Center for Biotechnology Information (NCBInr); taxonomy, all entries; enzyme, Lys-C (0 missed cleavages); fixed modification, pyridylethyl (C); variable modification, oxidation (M); peptide tol., ±300 ppm.

■ ASSOCIATED CONTENT

Supporting Information

Description of the material. This material is available free of charge via the Internet at http://pubs.acs.org.

■ AUTHOR INFORMATION

Corresponding Author

*E-mail: hnagaoka@sanyofoods.co.jp.

Notes

The authors declare no competing financial interest.

■ ACKNOWLEDGMENTS

We thank Prof. Kohtaro Kirimura and Keisuke Udagawa from Waseda University for the valuable advice and warm encouragement, and we thank GM. Koh Ueda from Wako Pure Chemical Industries, Ltd. for placing SanCat-*R* on the market (i.e., the CMPX: Code No. 355-34211 (for 1g) and Code No. 351-34213 (for 5g), respectively).

■ REFERENCES

(1) (a) Auld, D. S.; Bergman, T. *Cell. Mol. Life Sci.* **2008**, *65*, 3961−3970. (b) Giles, M. N.; Watts, B. A.; Giles, I. G.; Fry, H. F.; Littlechild, A. J.; Jacob, C. *Chem. Biol.* **2003**, *10*, 677−693. (c) Giles, M. N.; Giles, I. G.; Jacob, C. *Biophys. Res. Commun.* **2003**, *300*, 1−4.

(2) (a) Sobolov, B. S.; Leonida, D. M.; Malik, B. A.; Voivodov, I. K.; McKinney, F.; Kim, J.; Fry, J. *J. Org. Chem.* **1996**, *61*, 2125−2128. (b) Kamezawa, M.; Kitamura, M.; Nagaoka, H.; Tachibana, H.; Ohtani, T.; Naoshima, Y. *Liebigs Ann.* **1996**, *1996*, 167−170. (c) Schoemaker, H. E.; Mink, D.; Wubbolts, M. G. *Science* **2003**, *299*, 1694−1697. (d) Egami, H.; Katsuki, T. *J. Am. Chem. Soc.* **2007**, *129*, 8940−8941.

(3) (a) Lee, D. S.; Yamada, H.; Sugimoto, H.; Matsunaga, I.; Ogura, H.; Ichihara, K.; Adachi, S.; Park, S. Y.; Shiro, Y. *J. Biol. Chem.* **2003**, *278*, 9761−9767. (b) Shoji, O.; Fujishiro, T.; Nakajima, H.; Kim, M.; Nagano, S.; Shiro, Y.; Watanabe, Y. *Angew. Chem., Int. Ed.* **2007**, *46*, 3656−3659. (c) Yosca, T. H.; Rittle, J.; Krest, C. M.; Onderko, E. L; Beham, A.-R. K.; Green, M. T. *Science* **2013**, *342*, 825−829. (d) Ortiz de Montellano, P. R., Ed. *Cytochrome P450: Structure, Mechanism, and Biochemistry*, 3rd ed.; Kluwer Academic/Plenum: New York, Boston, Dorcrecht, London, Mosow, 2004. (e) Prage, B. E.; Pawelzik, S.-C.; Busenlehner, S. L.; Kim, K.; Morgenstern, R.; Jakobsson, P.-J.; Armstrong, R. N. *Biochemistry* **2011**, *50*, 7684−7693. (f) Johansson, A.-L.; Carlsson, J.; Hogbom, M.; Hosler, J. P.; Gennis, R. B.; Brzezinski, P. *Biochemistry* **2013**, *52*, 827−836.

(4) (a) Oldham, M. L.; Khare, D.; Quiocho, F. A.; Davidson, A. L.; Chen, J. *Nature* **2007**, *450*, 515−521. (b) Krieg, S.; Huché, F.; Diederichs, K.; Izadi-Pruneyre, N.; Lecroisey, A.; Wandersman, C.; Delepelaire, P.; Welte, W. *Proc. Natl. Acad. Sci. U.S.A.* **2009**, *106* (4), 1045−1050. (c) Izadi-Pruneyre, N.; Wolff, N.; Redeker, V.; Wandersman, C.; Delepierre, M.; Lecroisey, A. *J. Bacteriol.* **1999**, *261*, 562−568. (d) Guengerich, F. P. *Chem. Res. Toxicol.* **2001**, *14*, 611−650. For more information on cytochrome p450 from a genomics perspective, please check the **Protein of the Month** at the European Bioinformatics Institute. (e) McDonald, A. R.; Bukowski, M. R.; Farquhar, E. R.; Jackson, T. A.; Koehntop, K. D.; Seo, M. S.; De Hont, R. F.; Stubna, A.; Halfen, J. A.; Muonck, E.; Nam, W.; Que, L., Jr. *J. Am. Chem. Soc.* **2010**, *132*, 17118−17129.

(5) (a) Nagaoka, H.; Kayahara, H. *Biosci. Biotechnol. Biochem.* **1999**, *63*, 1991−1992. (b) Nagaoka, H.; Kayahara, H. *Biosci. Biotechnol. Biochem.* **2000**, *64*, 781−784. (c) Nagaoka, H.; Kayahara, H.; Wakabayashi, Y. *Biosci. Biotechnol. Biochem.* **2001**, *65*, 634−637.

(6) (a) Nagaoka, H. *Biotechnol. Prog.* **2003**, *19*, 1149−1155. (b) Nagaoka, H. *Curr. Top. Nutraceutical Res.* **2003**, *1*, 281−288. (c) Nagaoka, H. *Biotechnol. Prog.* **2004**, *20*, 128−133. (d) Nagaoka, H. *Biotechnol. Prog.* **2005**, *21*, 405−410.

(7) Nagaoka, H.; Udagawa, K.; Kirimura, K. *Biotechnol. Prog.* **2012**, *28*, 953−961.

(8) Thakur, V. V.; Sudalai, A. *Indian J. Chem.* **2005**, *44B*, 557−561.

(9) Paulsen, I. T.; Press, C. M.; Ravel, J.; Kobayashi, D. Y.; Myers, G. S.; Mavrodi, D. V.; DeBoy, R. T.; Seshadri, R.; Ren, Q.; Madupu, R.; Dodson, R. J.; Durkin, A. S.; Brinkac, L. M.; Daugherty, S. C.; Sullivan, S. A.; Rosovitz, M. J.; Gwinn, M. L.; Zhou, L.; Schneider, D. J.; Cartinhour, S. W.; Nelson, W. C.; Weidman, J.; Watkins, K.; Tran, K.; Khouri, H.; Pierson, E. A.; Pierson, L. S, 3rd.; Thomashow, L. S.; Loper, J. E. *Nat. Biotechnol.* **2005**, *23* (7), 873−878.

(10) (a) Cope, L.; Thomas, S.; Hrkal, Z.; Hansen, E. *Infect. Immun.* **1998**, *66*, 4511−4516. (b) Wandersman, C.; Stojiljkovic, I. *Curr. Opin. Microbiol.* **2000**, *3*, 215−220.

(11) (a) Braun, V.; Killmann, H. *Trends Biochem. Sci.* **1999**, *24*, 104−109. (b) Létoffé, S.; Omori, K.; Wandersman, C. *J. Bacteriol.* **2000**, *182* (16), 4401−4405.

(12) (a) Ghigo, J. M.; Létoffé, S.; Wandersman, C. *J. Bacteriol.* **1997**, *179*, 3572−3579. (b) Cwerman, H.; Wanderson, C.; Biville, F. *J. Bacteriol.* **2006**, *188*, 3357−3364.

(13) Chimento, D. P.; Kadner, R. J.; Wiener, M. C. *Protein* **2005**, *59*, 240−251.

(14) Barjon, C.; Wecker, K.; Izadi-Pruneyre Delepelaire, P. *J. Bacteriol.* **2007**, *189*, 5379−5382.

(15) (a) Adam, W.; Boland, W.; Hartmann-Schreier, J.; Hump, H.-U.; Lazarus, M.; Saffert, A.; Saha-Moller, C. R.; Schreier, P. *J. Am. Chem. Soc.* **1998**, *120*, 11044. (b) Landwehr, M.; Hochrein, L.; Otey, R. C.; Kasrayan, A.; Bäckvall, E. J.; Arnold, H. F. *J. Am. Chem. Soc.* **2006**, *128*, 6058−6059.

(16) (a) Shimizu, H.; Schuller, D. J.; Lanzilotta, W. N.; Sundaramoorthy, M.; Arciero, D. M.; Hooper, A. B.; Poulos, T. L. *Biochemistry* **2001**, *40*, 13483. (b) Erman, J. E.; Vitello, L. B. *Biochem. Biophys. Acta* **2002**, *1597*, 193. (c) Liu, X.; Dong, Y.; Zhang, A.; Wang, L.; Feng, L. *Microbiology* **2009**, *155*, 2078. (d) Hays Putnam, A. M.; Lee, Y. T.; Goodin, D. B. *Biochemistry* **2009**, *48*, 1−3.
(17) Afolabi, P. R.; Mohammed, F.; Amaratunga, K.; Majekodunmi, S. L.; Dales, S. L.; Gill, R.; Thompson, D.; Cooper, J. B.; Wood, S. P.; Goodwin, P. M.; Anthony, C. *Biochemistry* **2001**, *40*, 9799−9808.
(18) (a) Zee, J. M.; Glerum, D. M. *Biochem. Cell Biol.* **2006**, *84*, 859−869. (b) Busenlehner, S. L.; Brndn, G.; Namslauer, I.; Brzezinski, P.; Armstrong, R. N. *Biochemistry* **2008**, *47*, 73−83.
(19) Protein sequence based on a BLAST query sequence analysis of Cycle No. for YP 262445.1 is available on the internet on NCBI resource: http://www.ncbi.nlm.nih.gov/protein/70732682) and the full length gene sequences is available to the web on PATRIC resource: VBIPseFlu72549_5489: http://patricbrc.vbi.vt.edu/portal/portal/patric/Feature?cType=feature&cId=19880237).